Non-Gaussian-state generation with time-gated photon detection

Tatsuki Sonoyama,[1,*] Kazuma Takahashi,[1] Baramee Charoensombutamon,[1] Sachiko Takasu,[2] Kaori Hattori,[2,3] Daiji Fukuda,[2,3] Kosuke Fukui,[1] Kan Takase,[1,4] Warit Asavanant,[1,4] Jun-ichi Yoshikawa,[4] Mamoru Endo,[1,4] and Akira Furusawa[1,4,†]

[1]*Department of Applied Physics, School of Engineering, The University of Tokyo, 7-3-1 Hongo, Bunkyo-ku, Tokyo 113-8656, Japan*
[2]*National Institute of Advanced Industrial Science and Technology, Tsukuba, Ibaraki 305-8563, Japan*
[3]*AIST-UTokyo Advanced Operando-Measurement Technology Open Innovation Laboratory, Tsukuba, Ibaraki 305-8563, Japan*
[4]*Optical Quantum Computing Research Team, RIKEN Center for Quantum Computing, 2-1 Hirosawa, Wako, Saitama 351-0198, Japan*

(Received 28 February 2023; revised 26 May 2023; accepted 25 July 2023; published 5 September 2023)

Non-Gaussian states of light, which are essential in fault-tolerant and universal optical quantum computation, are typically generated by a heralding scheme using photon detectors. Recently, it has been theoretically shown that the large timing jitter of the photon detectors deteriorates the purity of the generated non-Gaussian states [T. Sonoyama *et al.*, Phys. Rev. A **105**, 043714 (2022)]. Here, we circumvent this problem by time-gated photon detection and generate non-Gaussian states with Wigner negativity using continuous-wave light. We use a fast optical switch for time gating to effectively improve the timing jitter of a photon-number-resolving detector based on a transition edge sensor from 50 ns to 10 ns. As a result, we generate non-Gaussian states with Wigner negativity of -0.011 ± 0.004 ($\hbar = 1$), which cannot be observed without the time-gated photon detection method. These results confirm the effect of the timing jitter on non-Gaussian state generation experimentally for the first time. The proposed time-gated photon detection method would be useful for high-purity non-Gaussian state preparation in optical quantum information processing.

DOI: 10.1103/PhysRevResearch.5.033156

I. INTRODUCTION

Non-Gaussian states of light are important resources in various fields such as quantum metrology [1,2], quantum communication [3,4], and quantum computation [5–13]. Especially in the field of continuous-variable quantum information processing, quantum computation with Gaussian states and Gaussian operations have already been demonstrated [14–17], and the remaining issues are quantum computation with non-Gaussian states and non-Gaussian operations, which are necessary for fault tolerance and universality.

In the optical systems, non-Gaussian states are typically generated by a heralding scheme using entangled resource and photon detectors [18–21] as in Fig. 1. However, the purity of non-Gaussian states generated experimentally, which is crucial for their applications, is still limited because of the performances of photon detectors such as detection efficiency and photon-number-resolving ability. Recently, it has become theoretically clear that the timing jitter of the photon detector also affects the purity of the generated states when continuous-wave (CW) light is used [22]. In particular, when the magnitude of the timing jitter is large and non-negligible relative to the wave-packet width of the generated state, the timing of the state generation is unclear as shown in Fig. 1(a) and the purity is degraded. Most of the previous studies used single-photon detectors [23,24] with low timing jitter of less than 1 ns to generate states on wave packets of several tens of nanoseconds [25–28]. Thus, the effect of timing jitter was low enough to ignore. On the other hand, the use of photon-number-resolving detectors (PNRDs) is needed for generating more complex non-Gaussian states. The timing jitter of the typical PNRD based on transition edge sensors (TESs) [29] is about 50 ns, which is non-negligible compared to the typical wave-packet width of several tens of nanoseconds. Furthermore, considering its application in quantum computation, the wave-packet width is expected to become even shorter for ultrafast quantum computation. This is because the clock frequency of computation is limited by the wave-packet width when the time-domain multiplexing scheme is used, which is one of the promising methods of optical quantum computation [14–17]. Therefore, the relative magnitude of timing jitter to wave-packet width is expected to become larger and it has become necessary to deal with this problem of timing jitter in non-Gaussian state generation.

Here, we introduce time-gated photon detection using a high-speed optical switch to improve the timing jitter in non-Gaussian state preparation. In conventional photon detection, the output signal of the detector is used as a timing reference of the state generation as shown in Fig. 1(a). In this case, the temporal resolution is determined by the detector's timing jitter ΔT_p. On the other hand, in time-gated photon detection,

*sonoyama@alice.t.u-tokyo.ac.jp
†akiraf@ap.t.u-tokyo.ac.jp

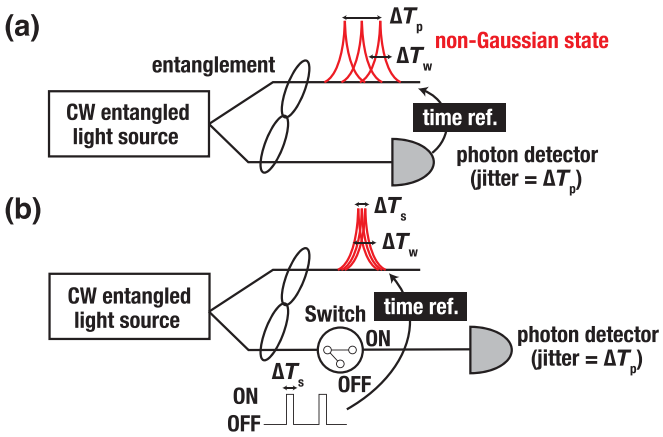

FIG. 1. Schematic diagram of non-Gaussian-state preparation by a heralding scheme using a CW entangled light source. (a) Conventional photon detection method. The detector's output is used as a time reference for determining state preparation timing. Thus, the temporal resolution is determined by the original timing jitter of photon detector ΔT_p. Here, we note that ΔT_w is the temporal width of the wave packet. (b) Time-gated photon detection method. An optical switch is put just before the photon detector and operated in a short time window. By using the driving signal as a time reference, the temporal resolution is determined by the time window ΔT_s, which becomes the effective timing jitter.

an optical switch is placed in front of the detector as shown in Fig. 1(b), which operates only for a short time ΔT_s to limit the photon detection time. By using the on/off signal of the optical switch as the reference signal for the state generation time, the temporal resolution is determined by the time window ΔT_s of the optical switch, which becomes the effective timing jitter. Thus, the timing jitter can be improved when the time window ΔT_s of the optical switch is shorter than the original timing jitter ΔT_p of the detector.

In this study, a Pockels cell and a polarizing beam splitter (PBS) are used as an optical switch, and the effective timing jitter of a TES is controlled by the time window of the optical switch. As a result, the timing jitter of the TES is improved from 50 ns to 10 ns, and a Schrödinger kitten state, one of the non-Gaussian states, with Wigner negativity of -0.011 ± 0.004 is successfully generated. This is in contrast with the case without time-gated photon detection, where the negative value of the Wigner function cannot be confirmed. There have been previous studies on Schrödinger kitten state generation using pulsed light sources and TESs [30–32], and using CW light sources and on-off detectors [21,26–28,33,34], but to our knowledge, this is the first Schrödinger kitten state generation using a CW light source and a TES. These results show the effect of timing jitter on the generated states experimentally and provide a promising method for generating high-purity non-Gaussian states.

II. TEMPORAL MODE FUNCTIONS OF OPTICAL QUANTUM STATES

The optical quantum states we are dealing with exist in a wave packet. By defining the temporal mode function $f(t)$ as the function that represents the temporal shape of the wave packet, the complex amplitude of the wave packet $\hat{a}_f$ is expressed using the amplitude $\hat{a}(t)$ of the electromagnetic field at time t as follows:

$$\hat{a}_f = \int_{-\infty}^{\infty} dt\, f(t)\hat{a}(t), \tag{1}$$

where $f(t)$ satisfies $\int_{-\infty}^{\infty} dt|f(t)|^2 = 1$. Here we consider rotating frame so that $f(t)$ does not include the oscillation components of the carrier frequency. Since the complex amplitude $\hat{a}_f$ is not an observable, the quadratures corresponding to the real and imaginary components $\hat{x}_f = \frac{\hat{a}_f + \hat{a}_f^\dagger}{\sqrt{2}}$, $\hat{p}_f = \frac{\hat{a}_f - \hat{a}_f^\dagger}{\sqrt{2}i}$ are used to describe quantum states. The quadratures satisfy the commutation relation $[\hat{x}_f, \hat{p}_f] = i$, where $\hbar$ is set to 1. In this paper, we denote the density matrix and the state vector of the quantum state excited on the temporal mode $f(t)$ as $\hat{\rho}_f$ and $|\psi\rangle_f$.

III. HERALDED GENERATION OF SCHRÖDINGER KITTEN STATES

In this experiment, a Schrödinger kitten state, which is a small Schrödinger cat state known as a fundamental element of optical quantum information processing, is chosen as a non-Gaussian state to be generated. The Schrödinger cat state is a superposition of a coherent state, i.e., $|\text{cat}\rangle = \frac{1}{N_{\psi,\alpha}}(|\alpha\rangle + e^{i\psi}|-\alpha\rangle)$, where ψ is the relative phase and $N_{\psi,\alpha}$ is a normalization constant. A Schrödinger kitten state can be generated approximately by subtracting a photon from the squeezed light [20,21,26–28,30–33].

Here, we discuss the effect of the timing jitter of photon detection on the quantum state generated by a CW light quantitatively. The theoretical analysis for the case of single-photon-state generation has been presented in Ref. [22], so in this paper we extend it to the case of Schrödinger-kitten-state generation as well. First, if the timing jitter is sufficiently low, it is known that the generated quantum state is expressed as follows [27,28]:

$$\hat{a}_{N(g)}\hat{S}_r|0\rangle \propto \hat{S}_r\hat{a}^\dagger_{N(g*r)}|0\rangle, \tag{2}$$

where $N(\cdot)$ is a normalizing operation, $g(t)$ is a time-reversed function of frequency filter's impulse response placed before photon detection, $r(t)$ is the time correlation function of the squeezed light, and $\hat{S}$ is a squeezing operator. By defining $f(t)$ as $g * r(t)$, this quantum state can be approximated as the Schrödinger kitten state $|\text{kitten}\rangle_f$. Frequency filters are used in order to limit the frequency bandwidth of photon detection and to increase the purity of the state. On the other hand, if the timing jitter is poor and its effect cannot be ignored, the quantum state generated is a mixture of Schrödinger kitten states excited on wave packets with different times, as shown in Fig. 1(a). Assuming the distribution function of timing jitter as $j(t)$, the generated state $\hat{\rho}$ can be expressed as follows:

$$\hat{\rho} \propto \int_{-\infty}^{\infty} dt'\, j(t')\,|\text{kitten}\rangle\langle\text{kitten}|_{f(t-t')}. \tag{3}$$

Such a quantum state $\hat{\rho}$ is a multimode state in multiple wave packets, but what we want to generate is a single-mode Schrödinger kitten state that can be used for quantum computation. We therefore consider choosing a temporal mode

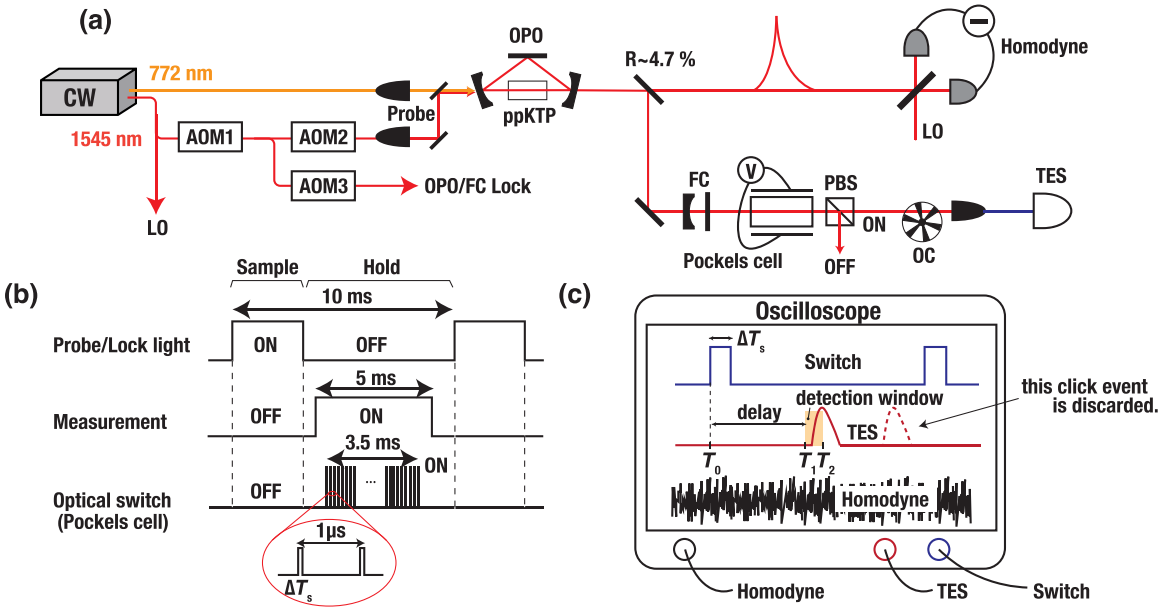

FIG. 2. (a) Simple schematic diagram of the experimental setup for Schrödinger-kitten-state generation with time-gated photon detection. An optical switch consists of a Pockels cell and a PBS. Here, a probe light and OPO/FC lock light are used for the feedback control of the phase and the cavity length. OPO: optical parametric oscillator (HWHM = 58.4 MHz), FC: filter cavity (HWHM = 8 MHz), ppKTP: periodically poled $KTiOPO_4$, LO: local oscillator, AOM: acousto-optic modulator, OC: optical chopper. (b) The measurement sequence. (c) The homodyne measurement setup of the time-gated photon detection method. The measurement is triggered only when the TES's signal rises within the detection time window from T_1 to T_2, whose timing reference is determined by the control signal of the optical switch. Here, the detection time window is determined considering a delay in the TES's signal relative to the on/off signal of the switch and the time window ΔT_s of the optical switch and the timing jitter of the TES.

$f_1(t)$ such that the quantum state on $f_1(t)$ is closest to the Schrödinger kitten state. This $f_1(t)$ can be obtained by a principal component analysis (PCA) method [22]. Then, the generated state $\hat{\rho}_{f_1}$ in the temporal mode $f_1(t)$ can be expressed as follows using the Schrödinger kitten state $|\text{kitten}\rangle$ and the squeezed state $|\text{sqz}\rangle$:

$$\hat{\rho}_{f_1} = \lambda_1 |\text{kitten}\rangle \langle\text{kitten}|_{f_1} + (1-\lambda_1) |\text{sqz}\rangle \langle\text{sqz}|_{f_1}, \quad (4)$$

where the parameter λ_1 and the temporal mode function $f_1(t)$ depend on the ratio of the timing jitter to the time width ΔT_w of the original wave packet $f(t)$. When the timing jitter relative to ΔT_w is low enough, λ_1 approaches 1 and $f_1(t)$ approaches $g * r(t)$. On the other hand, when the timing jitter becomes worse, λ_1 becomes smaller and $f_1(t)$ becomes wider in time. Thus, the generated quantum state becomes a mixture of the Schrödinger kitten state (non-Gaussian state) and the squeezed state (Gaussian state).

The timing jitter dependence on the generated quantum states can be confirmed experimentally. First, the optimal temporal mode $f_1(t)$ can be obtained by the PCA method, and the timing jitter's effect is confirmed by seeing how the shape of $f_1(t)$ changes with the magnitude of the timing jitter. In addition, the purity of the quantum state, which is related to λ_1 in Eq. (4), can be confirmed from the photon number distribution of the generated quantum states and the value of the Wigner function near the origin. This is because the squeezed light has an even-photon nature and the Schrödinger kitten state generated by the single-photon subtraction in this experiment has an odd-photon nature [19], and the value at the origin of the Wigner function is $-\frac{1}{\pi}$ for a quantum state with odd-photon nature and $\frac{1}{\pi}$ for a quantum state with even-photon nature [35,36]. In this paper, these properties are used to evaluate the generated quantum states.

IV. EXPERIMENTAL SETUP

In this experiment, Schrödinger kitten states are generated by photon subtraction both with and without the optical switch for comparison. In particular, five patterns are performed with the optical switch (time window of 10, 30, 50, and 70 ns) and without the optical switch (the original timing jitter of the TES is $\Delta T_p = 58$ ns, which is estimated experimentally).

The experimental setup is shown in Fig. 2(a), where the light source is a CW laser at 1545.32 nm and the squeezed light is generated by an optical parametric oscillator (OPO) whose half-width-at-half-maximum (HWHM) linewidth is 58 MHz. A small portion of the generated squeezed light is reflected by a beam splitter and a single photon is detected by the TES after a frequency filtering whose HWHM is 8 MHz. These frequency parameters determine the wave-packet width ΔT_w of the generated state when the timing jitter of photon detection can be neglected. The theoretically expected value is about $\Delta T_w = 22$ ns. A Pockels cell and a PBS are used as an optical switch and the minimum time window of this optical switch is 10 ns, which is small compared to the temporal width of the wave packet ΔT_w. The Pockels cell used in this study is $RTiOPO_4$, which has the extinction ratio of more than 30 dB and the transmittance of more than 95%. The Pockels cell driver, which drives the voltage applied to the Pockels cell, has a rise time of about 3.5 ns and a maximum repetition rate

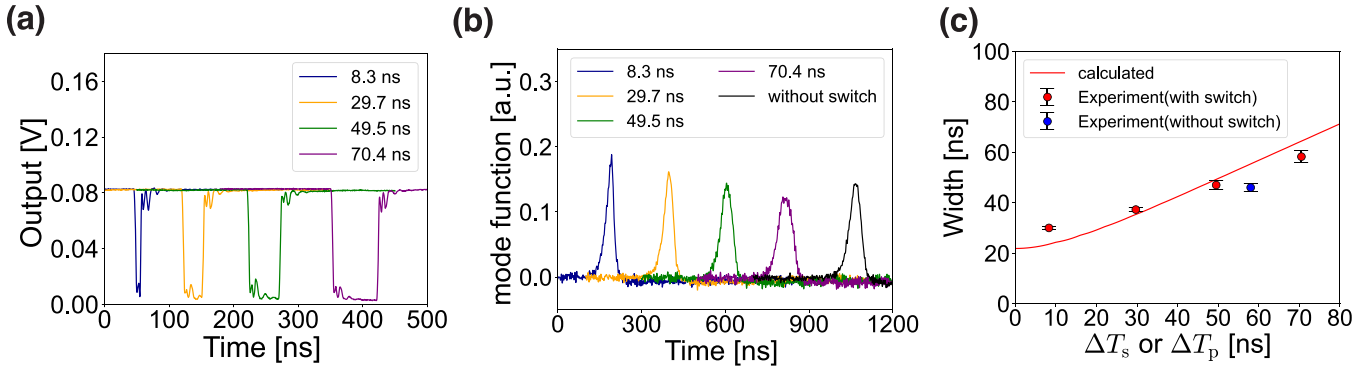

FIG. 3. (a) Response of the optical switch to an input of classical light. To improve visibility, each signal has different offsets in the horizontal axis. (b) The estimated temporal mode functions $f_1(t)$ of the generated quantum states. Here, when the optical switch is not used, the timing jitter is TES's original jitter $\Delta T_p = 58$ ns. As in (a), each signal has different offsets. (c) The plots of the time width (FWHM) of the estimated temporal mode functions and the time width (FWHM) of the theoretically calculated temporal mode functions. ΔT_w corresponds to the time width when the timing jitter ΔT_p or ΔT_s is 0. As mentioned earlier, even if ΔT_s is larger than the original photon detector timing jitter, the effective timing jitter is determined by the optical switch time window ΔT_s because the homodyne signal is triggered by the control signal of optical switch. Therefore, the horizontal axis ΔT_s or ΔT_p means the effective timing jitter. In the numerical calculations, the bandwidth of the OPO (HWHM) and the bandwidth of the filter cavity (HWHM) are assumed to be 58.4 MHz and 8 MHz, respectively. The distribution function of the timing jitter $j(t)$ is assumed to be a rectangular function. Here, the bootstrap method is used to obtain the error of the temporal mode function estimation.

of 1.2 MHz. The loss of the entire photon detection path is affected by the efficiency of the Pockels cell as well as the fiber coupling efficiency, the frequency filter's efficiency, and the detection efficiency of the TES. Since the detection efficiency of the TES is 62%, the efficiency of the entire photon detection path is lower than that, which leads to detection errors in which multiple photons are mistakenly detected as a single photon. This effect can be neglected by reducing the reflectance of the beam splitter for photon subtraction to lower the prior probability of multiple-photons subtraction, but on the other hand, the lower reflectance of the beam splitter leads to a reduction in the heralded event rates. Therefore, in this experiment, the reflectance is experimentally determined to be 4.7% in consideration of this trade-off.

The experimental measurement procedure is shown in Fig. 2(b). In this measurement, a sample-and-hold method is used, which is often used in experiments of non-Gaussian state generation [27,28,32,36]. In this method, the time for feedback control of phases and cavity lengths (sample) and the time for measurement of quantum states (hold) are periodically repeated. In the sample time, the classical light called a probe/lock light is used for feedback control. And in the hold time, the feedback control is held and the classical light is cut off to prevent it from being detected by the photon detector during the measurement. Here, acousto-optic modulators and an optical chopper are used for chopping the classical light. The sample-and-hold frequency is set at 100 Hz. The optical switch for time-gated photon detection is operated at a repetition frequency of 1 MHz, and switched on and off 3500 times during one measurement time of the sample-and-hold.

Here, the trigger signal of homodyne measurement that serves as a timing reference for the state generation is different when the optical switch is used and when the optical switch is not used. When the optical switch is not used, homodyne measurements are performed using the output signal of the TES as the measurement trigger. On the other hand, when the optical switch is used, homodyne measurements are performed using the operating signal of the optical switch as the measurement trigger only if the TES detects a photon while the optical switch is on. Experimentally, a detection window as shown in Fig. 2(c) is set on the oscilloscope, and homodyne measurement results are acquired only when the TES detection signal rises within that time window.

For verification, quadratures of the generated quantum states at time t, $\hat{x}_\theta(t) = \hat{x}(t)\cos\theta + \hat{p}(t)\sin\theta$, $(\theta = 0, \frac{1}{6}\pi, \frac{1}{3}\pi, \frac{1}{2}\pi, \frac{2}{3}\pi, \frac{5}{6}\pi)$ are obtained by homodyne measurements, from which the temporal mode functions and Wigner functions of the generated states are reconstructed. The loss of the signal path is estimated to be around 13% in total, which includes the loss inside the OPO (3.9%), the propagation loss (2.6%), the mode mismatching with the LO light (2.4%), and the efficiency of the photodetector (5.0%). Here we note that this 13% loss does not include the effective loss due to the photon detector's dark counts, finite timing jitter, and the contamination of multiple-photons subtraction events. The heralded event rates in this experiment are 17 s^{-1} (with the switch, 10 ns), 52 s^{-1} (30 ns), 79 s^{-1} (50 ns), 108 s^{-1} (70 ns), and 3900 s^{-1} (without the switch), respectively. The large difference in the heralding event rates with and without the optical switch is caused by the duty cycle of an optical switch. The dark count rates are less than 1% of the heralded event rates in all cases.

V. EVALUATION

The first step is to check the operation of the optical switch. Classical coherent light is injected into the optical switch, and a fast photodetector is placed immediately after the PBS to check its response. Figure 3(a) shows the response of the optical switch when the time window is set to

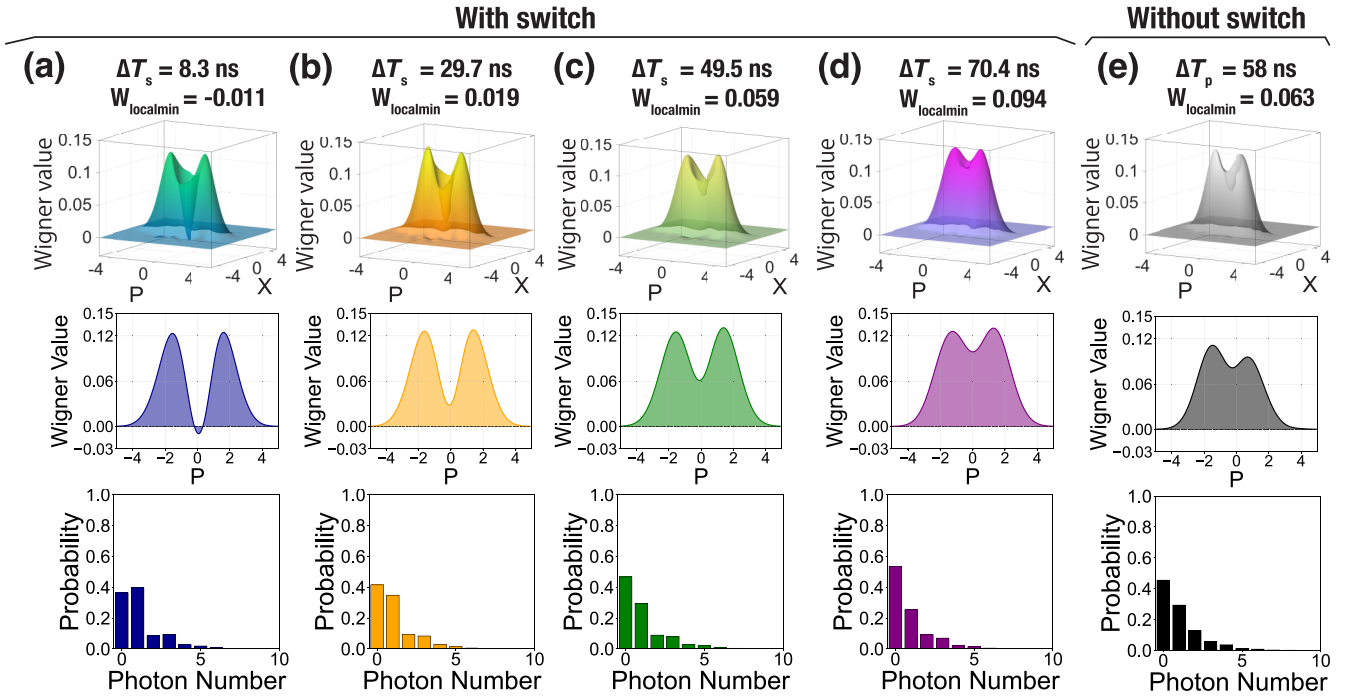

FIG. 4. (a–e) The reconstructed Wigner functions, their cross sections at $X = 0$, and photon number distributions with the optical switch ($\Delta T_s = 8.3$, 29.7, 49.5, and 70.4 ns) and without the optical switch ($\Delta T_p = 58$ ns). The local minimums around the origin of the Wigner functions are -0.011 ± 0.004, 0.019 ± 0.004, 0.059 ± 0.004, 0.094 ± 0.003 ($\Delta T_s = 8.3$, 29.7, 49.5, and 70.4 ns), and 0.063 ± 0.003 ($\Delta T_p = 58$ ns), respectively. The bootstrap method is also used to obtain the estimation error. We note that the minimum value near the origin and the value at the origin differ slightly in these reconstructed Wigner functions.

10, 30, 50, and 70 ns, respectively. The actual time widths are $\Delta T_s = 8.3$, 29.7, 49.5, and 70.4 ns, which are consistent with the set values. Here we note that even if ΔT_s is larger than ΔT_p, the effective timing jitter is determined by ΔT_s, not ΔT_p, because the control signal of the optical switch is used as a timing reference for the detection time in this experiment.

Next, the temporal mode functions of the generated quantum states are reconstructed. The temporal mode functions are obtained by PCA of the covariance matrix of the quadratures, taking advantage of the fact that the quadrature's variance of the generated quantum state is larger than the background quantum state [37,38]. Figure 3(b) shows the estimated temporal mode functions $f_1(t)$ of the generated states with and without the optical switch. This $f_1(t)$ corresponds to the first principal component obtained by PCA. Theoretically, as the timing jitter becomes worse, the width of the estimated temporal mode $f_1(t)$ should widen in time and its peak value should become smaller, and such a tendency is confirmed in Fig. 3(b). In addition, Fig. 3(c) compares experimental and numerically calculated theoretical values of the full-width-at-half-maximum (FWHM) of the temporal mode function $f_1(t)$ with respect to the timing jitter. The results with the optical switch are generally consistent with the theoretical line, but the result without the optical switch seems to deviate a little from the theoretical line. During the actual experiment, the waveform of TES's output signal may have changed slightly and the value of timing jitter may have changed due to environmental changes, which we consider as one possible cause of this difference. From these results, we confirm the improvement of the timing jitter and the change of the temporal mode function by time-gated photon detection.

Finally, the quadratures in the temporal mode $f_1(t)$ are calculated numerically as $\hat{x}_{f_1,\theta} = \int dt f_1(t)\hat{x}_\theta(t)$. Then, the density matrices and the Wigner functions are reconstructed from the quadrature data by quantum state tomography [39] without any loss correction. The reconstructed Wigner functions, their cross sections at $X = 0$, and the photon number distributions are shown in Fig. 4. As shown in Fig. 4(a), the Schrödinger kitten state with a negative value of -0.011 ± 0.004 near the origin is successfully generated when the time window of the optical switch is the shortest ($\Delta T_s = 8.3$ ns). The photon number distribution also confirms the odd-photon nature of the generated state, which is caused by subtracting a single photon from the squeezed state with even-photon nature. This shows that we succeed in generating a Schrödinger kitten state. Figures 4(b)–4(d) show that as the optical switch time window ΔT_s becomes wider (29.7 ns, 49.5 ns, and 70.4 ns), the value of the Wigner function near the origin gradually increases. Furthermore, Fig. 4(e) shows the Wigner function of the generated state without the optical switch ($\Delta T_p = 58$ ns) and the negative value near the origin cannot be observed here. From these results, we confirm that the improvement of timing jitter leads to the improvement of non-Gaussian states generation, as expected theoretically.

VI. DISCUSSION

The method of high-purity non-Gaussian state generation by time-gated photon detection can be applied to high-speed

optical quantum information processing from the following two points of view. The first point is that this method is applicable to non-Gaussian state generation with multiphoton detection, which is necessary for fault-tolerant optical quantum information processing. Since the optical switch with near unity switching efficiency is used, there is almost no reduction in photon detection efficiency and we believe that multiple-photon detection is possible in this scheme. The second point is that the wave packet of non-Gaussian states can be shortened to several picoseconds by using an ultrafast optical switch. The optical switch with a Pockels cell used in this paper has a gate time window of about 10 ns. On the other hand, the ultrafast optical switch using nonlinear optical effects demonstrated in Refs. [40,41] has a gate time window of less than 1 ps. Therefore, this method can reduce the timing jitter of the photon detector to less than 1 ps. This allows us to shorten the optical wave packet of non-Gaussian states to several picoseconds without degrading the purity. Since the wave-packet width determines the clock frequency of the optical quantum information processing, this method also contributes to speeding up the optical quantum information processing.

In this research we used a CW light source, but non-Gaussian state generation using a pulsed light source is also promising. Even when the pulsed light source is used, the purity of the generated state is still limited to some extent due to the timing jitter of photon detection because the state generation time generally depends on at which time within the pulse width the photon is detected. Here we believe that the proposed time-gated photon detection is also useful for improving the purity of non-Gaussian states when the pulsed light source is used if the optical switch's gate time is shorter than the pulse width. This is feasible if we use the subpicosecond optical switch mentioned earlier and the pulsed light with a duration time of several picoseconds. In non-Gaussian state generation using pulsed light, various methodologies have been proposed to achieve high purity, such as mode-selective photon subtraction [42,43], devising phase matching conditions [44], and using a frequency filter in photon detection [32,45]. And we believe that our method will be one of them.

VII. CONCLUSION

In this study, we introduce time-gated photon detection using a high-speed optical switch for non-Gaussian state generation. As a result, the effect of the timing jitter of the detector on the non-Gaussian state generation is experimentally clarified for the first time, and it is confirmed that the purity deteriorates when the timing jitter is non-negligibly large compared to the wave packet width of the generated state as expected theoretically. In addition, we improve the timing jitter of the PNRD-TES from 50 ns to 10 ns using this method, and succeed in generating a Schrödinger kitten state with a negative Wigner function value of -0.011. To the best of our knowledge, this is the first successful generation of a Schrödinger kitten state using a TES and a CW light source.

We believe that the non-Gaussian state generation method using time-gated photon detection proposed in this study would be a key technology to realize fault-tolerant, universal, and ultrafast optical quantum information processing.

ACKNOWLEDGMENTS

The authors acknowledge support from the UTokyo Foundation and donations from the Nichia Corporation of Japan. W.A. and M.E. acknowledge support from the Research Foundation for OptoScience and Technology. T.S., Kaz.T., and B.C. acknowledge financial support from the Forefront Physics and Mathematics Program to Drive Transformation (FoPM). The authors would like to thank Mr. Takahiro Mitani for careful proofreading of the manuscript. This work was partly supported by Japan Society for the Promotion of Science KAKENHI (Grants No. 18H05207, No. 20J10844, No. 20K15187, and No. 22K20351), Japan Science and Technology Agency Moonshot Research and Development (Grant No. JPMJMS2064), PRESTO (Grant No. JPMJPR2254), and CREST (Grant No. JPMJCR17N4).

[1] S. D. Huver, C. F. Wildfeuer, and J. P. Dowling, Entangled Fock states for robust quantum optical metrology, imaging, and sensing, Phys. Rev. A **78**, 063828 (2008).

[2] P. M. Anisimov, G. M. Raterman, A. Chiruvelli, W. N. Plick, S. D. Huver, H. Lee, and J. P. Dowling, Quantum Metrology with Two-Mode Squeezed Vacuum: Parity Detection Beats the Heisenberg Limit, Phys. Rev. Lett. **104**, 103602 (2010).

[3] R. Namiki, O. Gittsovich, S. Guha, and N. Lütkenhaus, Gaussian-only regenerative stations cannot act as quantum repeaters, Phys. Rev. A **90**, 062316 (2014).

[4] K. K. Sabapathy and A. Winter, Non-Gaussian operations on bosonic modes of light: Photon-added gaussian channels, Phys. Rev. A **95**, 062309 (2017).

[5] S. Lloyd and S. L. Braunstein, Quantum Computation over Continuous Variables, Phys. Rev. Lett. **82**, 1784 (1999).

[6] U. L. Andersen, J. S. Neergaard-Nielsen, P. van Loock, and A. Furusawa, Hybrid discrete- and continuous-variable quantum information, Nat. Phys. **11**, 713 (2015).

[7] D. Gottesman, A. Kitaev, and J. Preskill, Encoding a qubit in an oscillator, Phys. Rev. A **64**, 012310 (2001).

[8] P. T. Cochrane, G. J. Milburn, and W. J. Munro, Macroscopically distinct quantum-superposition states as a bosonic code for amplitude damping, Phys. Rev. A **59**, 2631 (1999).

[9] Z. Leghtas, G. Kirchmair, B. Vlastakis, R. J. Schoelkopf, M. H. Devoret, and M. Mirrahimi, Hardware-Efficient Autonomous Quantum Memory Protection, Phys. Rev. Lett. **111**, 120501 (2013).

[10] M. H. Michael, M. Silveri, R. T. Brierley, V. V. Albert, J. Salmilehto, L. Jiang, and S. M. Girvin, New Class of Quantum Error-Correcting Codes for a Bosonic Mode, Phys. Rev. X **6**, 031006 (2016).

[11] M. Bergmann and P. van Loock, Quantum error correction against photon loss using multicomponent cat states, Phys. Rev. A **94**, 042332 (2016).

[12] V. V. Albert, J. P. Covey, and J. Preskill, Robust Encoding of a Qubit in a Molecule, Phys. Rev. X **10**, 031050 (2020).

[13] A. L. Grimsmo, J. Combes, and B. Q. Baragiola, Quantum Computing with Rotation-Symmetric Bosonic Codes, Phys. Rev. X **10**, 011058 (2020).

[14] W. Asavanant, Y. Shiozawa, S. Yokoyama, B. Charoensombutamon, and A. Furusawa, Generation of time-domain-multiplexed two-dimensional cluster state, Science **366**, 373 (2019).

[15] M. V. Larsen, X. Guo, C. R. Breum, J. S. Neergaard-Nielsen, and U. L. Andersen, Deterministic generation of a two-dimensional cluster state, Science **366**, 369 (2019).

[16] W. Asavanant, B. Charoensombutamon, S. Yokoyama, T. Ebihara, T. Nakamura, R. N. Alexander, M. Endo, J. Yoshikawa, N. C. Menicucci, H. Yonezawa, and A. Furusawa, Time-Domain-Multiplexed Measurement-Based Quantum Operations with 25-MHz Clock Frequency, Phys. Rev. Appl. **16**, 034005 (2021).

[17] M. V. Larsen, X. Guo, C. R. Breum, J. S. Neergaard-Nielsen, and U. L. Andersen, Deterministic multi-mode gates on a scalable photonic quantum computing platform, Nat. Phys. **17**, 1018 (2021).

[18] C. K. Hong and L. Mandel, Experimental Realization of a Localized One-Photon State, Phys. Rev. Lett. **56**, 58 (1986).

[19] M. Dakna, T. Anhut, T. Opatrný, L. Knöll, and D.-G. Welsch, Generating Schrödinger-cat-like states by means of conditional measurements on a beam splitter, Phys. Rev. A **55**, 3184 (1997).

[20] A. Ourjoumtsev, T.-B. Rosa, L. Julien, and G. Philippe, Generating optical Schrdinger kittens for quantum information processing, Science **312**, 83 (2006).

[21] J. S. Neergaard-Nielsen, B. M. Nielsen, C. Hettich, K. Mølmer, and E. S. Polzik, Generation of a Superposition of Odd Photon Number States for Quantum Information Networks, Phys. Rev. Lett. **97**, 083604 (2006).

[22] T. Sonoyama, W. Asavanant, K. Fukui, M. Endo, J. Yoshikawa, and A. Furusawa, Analysis of optical quantum state preparation using photon detectors in the finite-temporal-resolution regime, Phys. Rev. A **105**, 043714 (2022).

[23] S. Cova, A. Longoni, and A. Andreoni, Towards picosecond resolution with single-photon avalanche diodes, Rev. Sci. Instrum. **52**, 408 (1981).

[24] B. Korzh, Q.-Y. Zhao, J. P. Allmaras, S. Frasca, T. M. Autry, E. A. Bersin, A. D. Beyer, R. M. Briggs, B. Bumble, M. Colangelo, G. M. Crouch, A. E. Dane, T. Gerrits, A. E. Lita, F. Marsili, G. Moody, C. Peña, E. Ramirez, J. D. Rezac, N. Sinclair *et al.*, Demonstration of sub-3 ps temporal resolution with a superconducting nanowire single-photon detector, Nat. Photonics **14**, 250 (2020).

[25] M. Yukawa, K. Miyata, T. Mizuta, H. Yonezawa, P. Marek, R. Filip, and A. Furusawa, Generating superposition of up-to three photons for continuous variable quantum information processing, Opt. Express **21**, 5529 (2013).

[26] K. Wakui, H. Takahashi, A. Furusawa, and M. Sasaki, Photon subtracted squeezed states generated with periodically poled $KTiOPO_4$, Opt. Express **15**, 3568 (2007).

[27] W. Asavanant, K. Nakashima, Y. Shiozawa, J. Yoshikawa, and A. Furusawa, Generation of highly pure Schrödinger's cat states and real-time quadrature measurements via optical filtering, Opt. Express **25**, 32227 (2017).

[28] K. Takase, A. Kawasaki, B. K. Jeong, M. Endo, T. Kashiwazaki, T. Kazama, K. Enbutsu, K. Watanabe, T. Umeki, S. Miki, H. Terai, M. Yabuno, F. China, W. Asavanant, J. Yoshikawa, and A. Furusawa, Generation of Schrödinger cat states with Wigner negativity using a continuous-wave low-loss waveguide optical parametric amplifier, Opt. Express **30**, 14161 (2022).

[29] D. Fukuda, G. Fujii, T. Numata, K. Amemiya, A. Yoshizawa, H. Tsuchida, H. Fujino, H. Ishii, T. Itatani, S. Inoue, and T. Zama, Titanium-based transition-edge photon number resolving detector with 98% detection efficiency with index-matched small-gap fiber coupling, Opt. Express **19**, 870 (2011).

[30] N. Namekata, Y. Takahashi, G. Fujii, D. Fukuda, S. Kurimura, and S. Inoue, Non-Gaussian operation based on photon subtraction using a photon-number-resolving detector at a telecommunications wavelength, Nat. Photonics **4**, 655 (2010).

[31] T. Gerrits, S. Glancy, T. S. Clement, B. Calkins, A. E. Lita, A. J. Miller, A. L. Migdall, S. W. Nam, R. P. Mirin, and E. Knill, Generation of optical coherent-state superpositions by number-resolved photon subtraction from the squeezed vacuum, Phys. Rev. A **82**, 031802(R) (2010).

[32] M. Endo, R. He, T. Sonoyama, K. Takahashi, T. Kashiwazaki, T. Umeki, S. Takasu, K. Hattori, D. Fukuda, K. Fukui, K. Takase, W. Asavanant, P. Marek, R. Filip, and A. Furusawa, Non-Gaussian quantum state generation by multi-photon subtraction at the telecommunication wavelength, Opt. Express **31**, 12865 (2023).

[33] M. Zhang, H. Kang, M. Wang, F. Xu, X. Su, and K. Peng, Quantifying quantum coherence of optical cat states, Photonics Res. **9**, 887 (2021).

[34] M. Takeoka, H. Takahashi, and M. Sasaki, Large-amplitude coherent-state superposition generated by a time-separated two-photon subtraction from a continuous-wave squeezed vacuum, Phys. Rev. A **77**, 062315 (2008).

[35] A. Royer, Wigner function as the expectation value of a parity operator, Phys. Rev. A **15**, 449 (1977).

[36] R. Nehra, A. Win, M. Eaton, R. Shahrokhshahi, N. Sridhar, T. Gerrits, A. Lita, S. W. Nam, and O. Pfister, State-independent quantum state tomography by photon-number-resolving measurements, Optica **6**, 1356 (2019).

[37] A. MacRae, T. Brannan, R. Achal, and A. I. Lvovsky, Tomography of a High-Purity Narrowband Photon from a Transient Atomic Collective Excitation, Phys. Rev. Lett. **109**, 033601 (2012).

[38] O. Morin, C. Fabre, and J. Laurat, Experimentally Accessing the Optimal Temporal Mode of Traveling Quantum Light States, Phys. Rev. Lett. **111**, 213602 (2013).

[39] A. I. Lvovsky and M. G. Raymer, Continuous-variable optical quantum-state tomography, Rev. Mod. Phys. **81**, 299 (2009).

[40] D. England, F. Bouchard, K. Fenwick, K. Bonsma-Fisher, Y. Zhang, P. J. Bustard, and B. J. Sussman, Perspectives on all-optical Kerr switching for quantum optical applications, Appl. Phys. Lett. **119**, 160501 (2021).

[41] C. Kupchak, J. Erskine, D. England, and B. Sussman, Terahertz-bandwidth switching of heralded single photons, Opt. Lett. **44**, 1427 (2019).

[42] V. Averchenko, C. Jacquard, V. Thiel, C. Fabre, and N. Treps, Multimode theory of single-photon subtraction, New J. Phys. **18**, 083042 (2016).

[43] Y.-S. Ra, A. Dufour, M. Walschaers, C. Jacquard, T. Michel, C. Fabre, and N. Treps, Non-Gaussian quantum states of a multimode light field, Nat. Phys. **16**, 144 (2020).

[44] K. Garay-Palmett, H. J. McGuinness, O. Cohen, J. S. Lundeen, R. Rangel-Rojo, A. B. U'Ren, M. G. Raymer, C. J. McKinstrie, S. Radic, and I. A. Walmsley, Photon pair-state preparation with tailored spectral properties by spontaneous four-wave mixing in photonic-crystal fiber, Opt. Express **15**, 14870 (2007).

[45] A. M. Brańczyk, T. C. Ralph, W. Helwig, and C. Silberhorn, Optimized generation of heralded Fock states using parametric down-conversion, New J. Phys. **12**, 063001 (2010).